Two Modes of Gating During Late Na^+ Channel Currents in Frog Sartorius Muscle

JOSEPH B. PATLAK and MAURICIO ORTIZ

From the Department of Physiology and Biophysics, University of Vermont, Burlington, Vermont 05405

ABSTRACT Na^+ currents were measured during 0.4-s depolarizing pulses using the cell-attached variation of the patch-clamp technique. Patches on Cs-dialyzed segments of sartorius muscle of *Rana pipiens* contained an estimated 25–500 Na^+ channels. Three distinct types of current were observed after the pulse onset: (*a*) a large initial surge of inward current that decayed within 10 ms (early currents), (*b*) a steady "drizzle" of isolated, brief, inward unitary currents (background currents), and (*c*) occasional "cloudbursts" of tens to hundreds of sequential unitary inward currents (bursts). Average late currents (background plus bursts) were 0.12% of peak early current amplitude at −20 mV. 85% of the late currents were carried by bursting channels. The unit current amplitude was the same for all three types of current, with a conductance of 10.5 pS and a reversal potential of +74 mV. The magnitudes of the three current components were correlated from patch to patch, and all were eliminated by slow inactivation. We conclude that all three components were due to Na^+ channel activity. The mean open time of the background currents was ~0.25 ms, and the channels averaged 1.2 openings for each event. Neither the open time nor the number of openings of background currents was strongly sensitive to membrane potential. We estimated that background openings occurred at a rate of 0.25 Hz for each channel. Bursts occurred once each 2,000 pulses for each channel (assuming identical channels). The open time during bursts increased with depolarization to 1–2 ms at −20 mV, whereas the closed time decreased to <0.2 ms. The fractional open time during bursts was fitted with m_∞^3 using standard Na^+ channel models. We conclude that background currents are caused by a return of normal Na^+ channels from inactivation, while bursts are instances where the channel's inactivation gate spontaneously loses its function for prolonged periods.

INTRODUCTION

The Na^+ channels that give rise to action potentials in nerve and muscle open transiently after membrane depolarization from the resting potential. The kinetics of this process have been studied extensively in squid axon, node of Ranvier, skeletal and cardiac muscle, and numerous other excitable cells (see French and

Address reprint requests to Dr. Joseph Patlak, Dept. of Physiology and Biophysics, University of Vermont, Given Bldg., Burlington, VT 05405.

J. GEN. PHYSIOL. © The Rockefeller University Press · 0022-1295/86/02/0305/22$1.00

Volume 87 February 1986 305–326

Horn, 1983, for a review). The currents through single Na^+ channels also have been measured in several cell types (for example, Sigworth and Neher, 1980; Patlak and Horn, 1982; Aldrich et al., 1983). Such studies have provided important new information about Na^+ channel function. Tetrodotoxin (TTX), which specifically blocks the Na^+ channel, also abolishes a relatively small inward current that slowly inactivates or remains steady during moderate, sustained depolarization in many preparations (Reuter, 1968; Shoukimas and French, 1980; Rakowski et al., 1985; Carmeliet, 1984). We refer to slowly inactivating and steady currents collectively as "late currents." One hypothesis advanced to explain late currents is that channels occasionally return from the inactivated to the open state, function normally for a short time, and then inactivate again (Hodgkin and Huxley, 1952; McAllister et al., 1975; Attwell et al., 1979). Another hypothesis postulates a second open state, which can only be reached from the inactivated state (Chandler and Meves, 1970; Bezanilla and Armstrong, 1977; Sigworth, 1981). Since both hypotheses predict specific channel behavior at late times, measurement of single channels during the late currents would help distinguish between these hypotheses.

If channels occasionally do return from the inactivated state, and if they have but one open state, then their activity should be the same during late currents as it was during the "early" currents at the start of the pulse. Measurements of late Na^+ channel currents would provide an independent check of hypotheses describing the early currents. Recent recordings of single Na^+ channels have shown that the activation is slower, and the inactivation quicker, than would be expected from classical models of Na^+ currents (Patlak and Horn, 1982; Aldrich et al., 1983). Aldrich et al. showed quantitatively that Na^+ channels inactivate quickly from the open state with a reaction rate that is largely independent of membrane potential. As a result, the dwell time in the open state is short, and channels seldom reopen. Other investigators, however, have observed more extensive channel reopening, as well as voltage dependence of the channel open time (Vandenberg and Horn, 1984). Measurement of the channels' open time and of their tendency to reopen before returning to the inactivated state during the late currents at various potentials might help to discriminate between the proposed kinetic schemes.

We recently reported that single Na^+ channels in cardiac muscle occasionally failed to inactivate, thus producing long bursts of openings (Patlak and Ortiz, 1985*b*). We speculated that these bursts might be due to channels functioning in a completely different kinetic mode, and that they might be the source of the late Na^+ currents. Less than 1% of our pulses contained late currents, however, and it was difficult to obtain sufficient quantitative information to determine their exact properties. Therefore, we sought to study Na^+ currents in a preparation with a high density of channels, in which events that were rare for an individual channel would be seen frequently enough to allow quantitative measurement of the single channel basis for the late Na^+ currents.

We report here the results of these experiments. We chose frog sartorius muscle, which has high Na^+ channel density. The high density allowed us to obtain patches with hundreds of Na^+ channels, and thus measure the late current.

Our results show that most of the late current is due to Na^+ channels that occasionally enter a kinetic "mode" where inactivation is markedly delayed. The remaining portion of the current appears to be carried by channels transiently returning from inactivation.

METHODS

Sartorius muscles from Vermont *Rana pipiens* were used for all studies, except where noted. The frogs were killed and the muscles were dissected using standard procedures. Muscles were pinned in a small dish and washed with "frog/saline" solution (in mM: 100 NaCl, 3 KCl, 0.2 $CaCl_2$, 1 $MgCl_2$, 5 HEPES, 5 glucose, pH 7.4). The frog/saline solution was exchanged with a low-Na^+ solution (in mM: 90 tetramethylammonium-Cl, 10 NaCl, 3 KCl, 0.2 $CaCl_2$, 1 $MgCl_2$, 5 HEPES, 5 glucose, pH 7.4) containing 3 mg/ml collagenase (type 1A, Sigma Chemical Co., St. Louis, MO). Muscles were bathed for 2–3 h at room temperature in this solution, rinsed, and bathed for 20 min in low-Na^+ solution containing 0.1 mg/ml protease (type VII, Sigma Chemical Co.). The muscles were rinsed a second time, and bathed in a "relaxing" solution (in mM: 95 Cs-aspartate, 3 $MgCl_2$, 5 Na_2ATP, 5 HEPES, 0.1 EGTA, pH 7.4) for 30 min. The fiber bundles were cut repeatedly in the transverse direction to produce many short segments of cut-open fibers, which were dispersed by trituration with a fire-polished Pasteur pipette.

The muscle segments were transferred to the recording chamber, allowed to settle, and washed with fresh relaxing solution. Most fiber segments were ~1–2 mm long. They had clear striations over most of their length, but they progressively disorganized at the opened ends over the course of several hours. We saw no tendency for the cut ends to reseal in the relaxing solution that we used. All experiments were performed with a static bath that was cooled to 10 ± 1 °C using a Peltier element mounted near the chamber.

Patch electrodes were made from Corning type 7052 glass (Corning Glass Works, Corning, NY), and were filled with frog/saline solution. The electrode was placed on the cell ~500 μm from the cut end of the fiber, and was pushed onto the membrane until a slight dimpling was observed. Gigohm seals were attained quickly in most cells after application of gentle suction. The patch electronics were standard (Hamill et al., 1981). The analog output signal was filtered with an eight-pole Bessel filter.

A Northstar (Berkeley, CA) microcomputer was used to control the pulse protocol and sample the patch currents. The fast phases of the currents were recorded at low gain (0.1 V/pA) during ensembles of 50–300 identical 5-ms test pulses delivered at 1 Hz. The data were filtered at 5 kHz, and sampled at 33-μs intervals. Slow currents were measured at high gain (1 V/pA) using 0.4-s test pulses, which were delivered sequentially to −50, −40, −30, and −20 mV at 10-s intervals. The pulse sequence was repeated continuously until the patch became unstable. Currents were filtered at 2 kHz and sampled at 100-μs intervals before, during, and after the pulses, and stored on floppy disk for later analysis. Capacity transients were reduced with an analog compensation circuit, and canceled digitally using appropriately scaled hyperpolarizing pulses.

The patch currents following depolarizing pulses consisted of three distinct types of activity. An initial surge of inward current decayed within 10 ms to a fine "drizzle" of openings that were superimposed on occasional "cloudbursts," which consisted of tens to hundreds of sequential openings. The amplitudes of the single channel events that gave rise to these currents were measured with three different techniques, as shown in Fig. 1. To measure the unit current amplitude during the fast surge, we used an ensemble fluctuation analysis similar to that of Sigworth (1980). Plots of the variance vs. mean current were made for all time points during the pulse, as shown in Fig. 1*A*. The resultant data were fitted by regression analysis with curves of the form

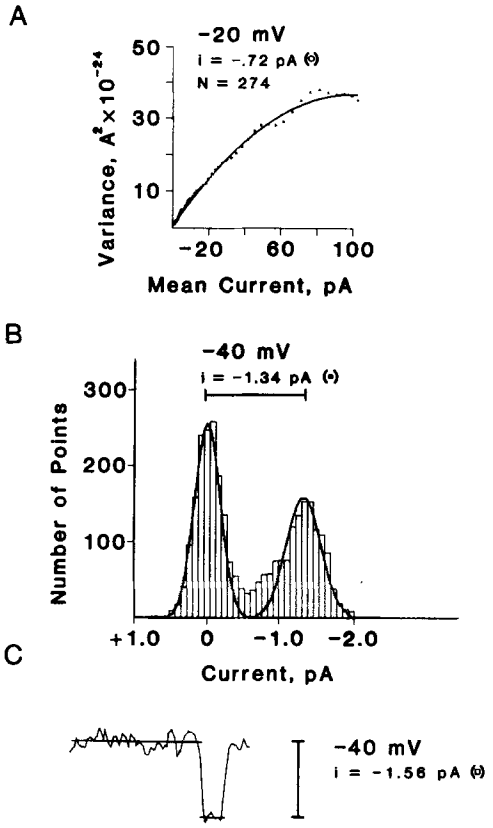

FIGURE 1. Three methods were used to measure the single channel amplitudes during the early, the burst, and the background currents. (*A*) Analysis of current fluctuations during pulse ensembles was used to measure the early unit current and the number of channels in a patch. The variance of the current at each time point is plotted (points) against the mean current at that time for an ensemble of 309 pulses (5 ms duration) to −20 mV from a holding potential of −120 mV. The data were fitted with a theoretical curve under the assumption of identical independent channels (see text). The best fit for the data shown in the figure is the solid curve, which corresponded to a unit current amplitude of −0.72 pA and 274 channels in the patch. The open circle indicates the symbol used to plot the resultant amplitudes in Fig. 4. (*B*) Histogram of current amplitudes during one burst. Each entry was the amplitude of current measured at 0.1-ms intervals during the 400-ms pulse. When no channel was bursting, the resultant histogram was well fitted by a single Gaussian curve with a mean of 0 pA (i.e., the baseline) and a standard deviation equal to the rms noise amplitude during the pulse. When a bursting channel was present, as in the example shown here, a second Gaussian component was present, corresponding to the level of the open channel. The data shown were for a burst during a pulse to −40 mV from a holding potential of −120 mV. The difference between the means of the two fitted Gaussian curves was taken as the best estimate of single channel current, −1.34 pA in this example. The solid circle indicates the symbol used to plot this type of measurement in Fig. 4. (*C*) Direct measurements of the difference between baseline and open channel current were used to estimate the amplitude of the background currents. The difference between the average current before and during the opening was determined to estimate the channel current amplitude. Each open square in Fig. 4 is the average of 30–50 such individual measurements made during five sequential pulses to the same potential.

$$\sigma^2 = i\bar{I} - \bar{I}^2/N,$$

where i is the current through one channel, $\bar{I}$ is the mean current at any time point, and N is the number of channels in the patch. The standard error of the parameters for these fits was large when ensembles contained fewer than 100–200 pulses. We report, therefore, only the fluctuation analyses from ensembles with 300 or more pulses.

The average amplitudes of the channel currents during each burst were determined by assembling a histogram of the current magnitude at every time point during the pulse, as shown in Fig. 1 *B*. In cases where channel activity was low, this histogram was well fitted by a single Gaussian curve. We assumed that the mean of this Gaussian was the level of zero current, i.e., the baseline. The standard deviation of ~0.2 pA was equal to the background rms noise amplitude during the pulse. A second Gaussian component was prominent during pulses in which bursting currents were present, as shown in the figure. These histograms were fitted (by eye) with the sum of two Gaussian curves. The difference between the mean levels of the two Gaussian components was taken as the best estimate of the single channel amplitude during that burst.

Finally, the amplitude of nonbursting late currents was measured directly, as shown in Fig. 1 *C*. The difference between the average current during an individual channel opening and the preceding baseline was measured. These measurements were repeated for each opening. 30–50 values thus obtained during five sequential pulses to the same potential were averaged to provide each estimate of the channel current.

The kinetics of channel activity for late times were determined with a semiautomated routine for detecting channel currents. The program determined the beginning and the end of individual openings based on the half-amplitude crossing criteria (Colquhoun and Sigworth, 1983). It did so sequentially for short segments of the data traces, condensing the actual data into strings of open and closed time durations. The program presented both data and idealized records for operator approval or modification. In instances where overlapping currents were detected, the durations of both openings were dropped from subsequent analyses. Histograms of channel open and closed times were generated from the idealized records. The histograms were fitted with one or two exponentials using a general nonlinear least-squares fitting routine. All deviations were weighted by the inverse of the number of elements in the bin (except bins with zero entries, which were weighted as if they had one entry).

Opening or closing events that were shorter than 0.1 ms could not be observed because of the limited frequency response of our recordings. If a short closing separated two openings, then our measurements would have erroneously counted a single opening that had a duration equal to the sum of the two actual open times, thus increasing our estimates of the mean open times for all events. Similarly, missed openings increase the estimates of channel closed times. Several techniques are available to correct the estimates of open and closed times (Neher, 1983; Colquhoun and Sigworth, 1983) if the form of their parent distributions is known, and if they are both significantly longer than the limit of resolution of the measurements. Unfortunately, our measurements could not always satisfy these requirements. In particular, the uncorrected time constants for both the open and closed time distributions were often fast enough to prevent explicit solution of the equations for correction. Therefore, the time constants that we report are uncorrected, and must be interpreted as upper bounds for the exact values of the parameters involved.

RESULTS

High Density of Na^+ Channels in Tight Patches

Frog sartorius muscle was chosen because it has a high density of Na^+ channels in its sarcolemma. Peak Na^+ currents were between 5 and 200 pA in our patches. Assuming a 2-μm^2 patch area, the peak current density was 0.25–10 mA/cm^2.

These estimates agree well with loose-patch measurements on similar preparations (Almers et al., 1983*a*; Roberts and Almers, 1985). Since our studies required high channel density, we selected patches with large peak Na^+ currents. We report here the results from 15 such patches that we have studied in depth.

The mean currents (average of 44 pulses) from one patch at seven different test pulse potentials are shown in Fig. 2. These currents have the same form as the currents measured from this preparation using vaseline-gap or loose-patch techniques (Hille and Campbell, 1976; Stuhmer et al., 1983). Even though the currents were quite large for cell-attached recordings, series resistance should not have had a significant influence on the records. The maximum voltage error

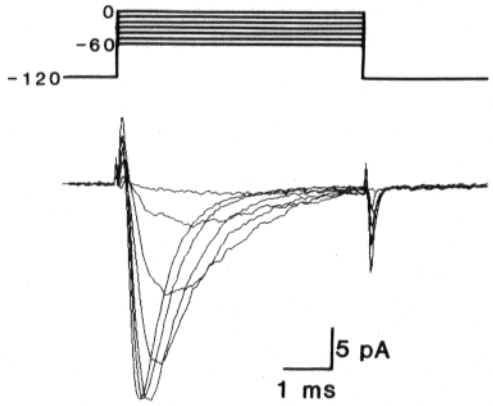

FIGURE 2. Mean early currents through Na^+ channels. Each trace on the lower part of the figure is the average of 44 current recordings obtained during consecutive identical pulses given from a holding potential of −120 mV. The seven pulse potentials used ranged from −60 to 0 mV, as indicated by the traces at the top of the figure, which represent the voltage pulses applied to the patch electrode. Since the cell segments were cut open and dialyzed with the bathing solution, they had no resting potentials. Thus, the voltages reported in this figure and elsewhere are absolute transmembrane potentials.

at the peak of the current should have been <2 mV, even with patch pipette series resistances as high as 10 MΩ.

Late Channel Openings Were Na^+ Currents

Inactivation of Na^+ channels was nearly complete after 10 ms at test pulse potentials more positive than −50 mV. Even in patches with hundreds of channels, the individual channel openings could be easily discerned after this time because the probability of two or more overlapping openings became very low, and because our limits of resolution were essentially the same as for any other gigohm seal recording. Fig. 3 shows the late currents during 10 long pulses to −40 mV. The fast currents, which had a peak amplitude of 45 pA and which are truncated in this high-gain recording, are seen as a gap at the start of the records.

Subsequent channel activity occurred with two distinct types of kinetics. The

first, which we call background current, can be seen in all pulses. This background activity consisted of short openings, most of which occur as isolated events. The second type of activity, which is prominent in the first and in the seventh through ninth pulses, consisted of prolonged bursts of openings. The overlapping events seen during most bursts fit the pattern of the background current. Bursts rarely were seen to overlap one another. Therefore, individual bursts were probably due to the activity of one channel.

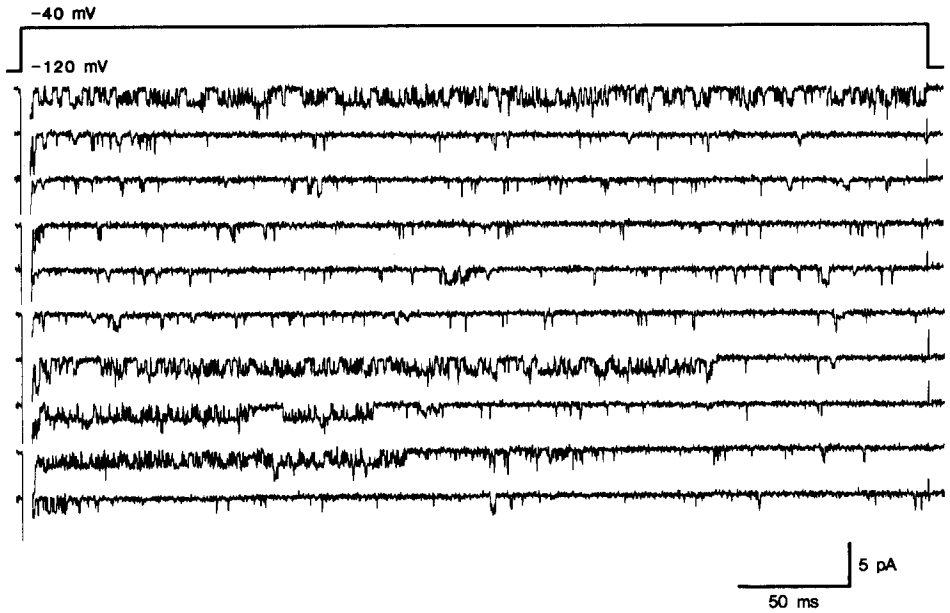

FIGURE 3. Late currents through Na^+ channels. The currents during 10 sequential 400-ms pulses are shown. The top trace represents the voltage pulse to −40 mV from a holding potential of −120 mV. The initial surge of current, similar to those in Fig. 2, reached −45 pA during these pulses. The early currents are truncated in these high-gain records, and are seen as gaps near the start of the pulse. Subsequent activity consisted of many individual "background" openings, present in all pulses, and occasional "bursts" of sequential openings, as seen in the first and the seventh through ninth pulses. The frequency of bursting is higher in this sequence, which was selected to illustrate both types of activity, than the average for the patch shown.

These two types of late currents were the result of Na^+ channel activity. The possible contribution of most other channels can be ruled out on the basis of single channel amplitude and polarity. For example, Ca^{2+} channels, under the conditions that we used, would have had single channel currents of $\ll$0.1 pA, and could not have been resolved. Delayed rectifier K^+ channels were present in patches obtained during preliminary experiments on cells that were not dialyzed with Cs^+. These K^+ channel currents, however, had opposite polarity from the late currents that we describe, and were blocked by Cs^+ under our recording conditions.

The amplitudes of the channel events that made up the fast currents, the background currents, and the bursts were not significantly different from one another. Fig. 4 shows the results of our measurements of channel amplitude on the 15 patches that we analyzed. Each solid circle indicates the mean amplitude of openings during an individual burst, using the method shown in Fig. 1*B*. Each open square is the average of 30–50 background current amplitudes at the same four potentials (the method shown in Fig. 1*C*). Each open circle in the figure is the value of the unitary current amplitude underlying the fast currents of one patch, determined using fluctuation analysis as illustrated in Fig. 1*A*. The fluctuation data are limited to measurements at −20 mV and one point at −40

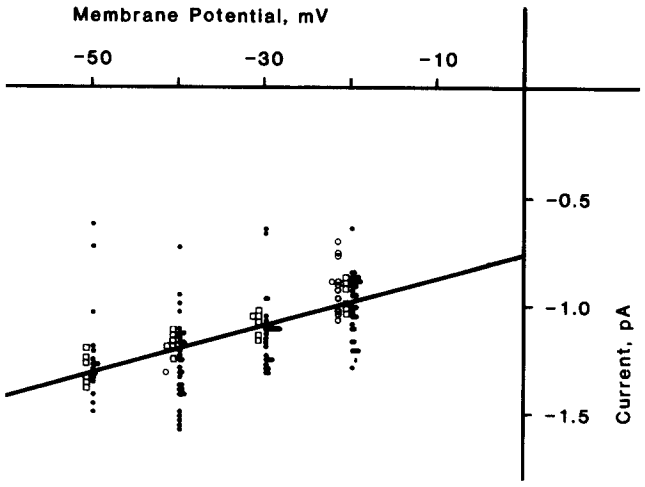

FIGURE 4. Single channel amplitudes for early, background, and burst currents as a function of membrane potential. Open circles represent values obtained from early currents using fluctuation analysis (see Fig. 1*A* and Methods). Each solid circle is the amplitude of the channel currents during one burst, obtained with the method described in Fig. 1*B*. The amplitudes of the background currents are indicated by the open squares, each of which is the average of 30–50 values measured as described in Fig. 1*C*. The solid line is a linear regression fit to all the points. It has a slope of 10.5 pS and crosses the abscissa at +74 mV.

mV because our fast current measurements at other potentials had an insufficient number of pulses. It is clear that the three types of measurement, each with its own sources of error, yield estimates of single channel current amplitude that overlap extensively. The measured values are consistent with the hypothesis that the currents were through Na^+ channels. The solid line in Fig. 4 is a linear regression using all of the data weighted equally. Its slope is 10.5 pS, and its extrapolated zero-current intercept is +74 mV.

The frequency of appearance of both the burst and the background currents in each patch was proportional to the magnitude of the peak mean current in that patch, as shown in Fig. 5. Fig. 5*A* plots the average number of background openings observed during 400-ms pulses in each of 15 patches. Since no signifi-

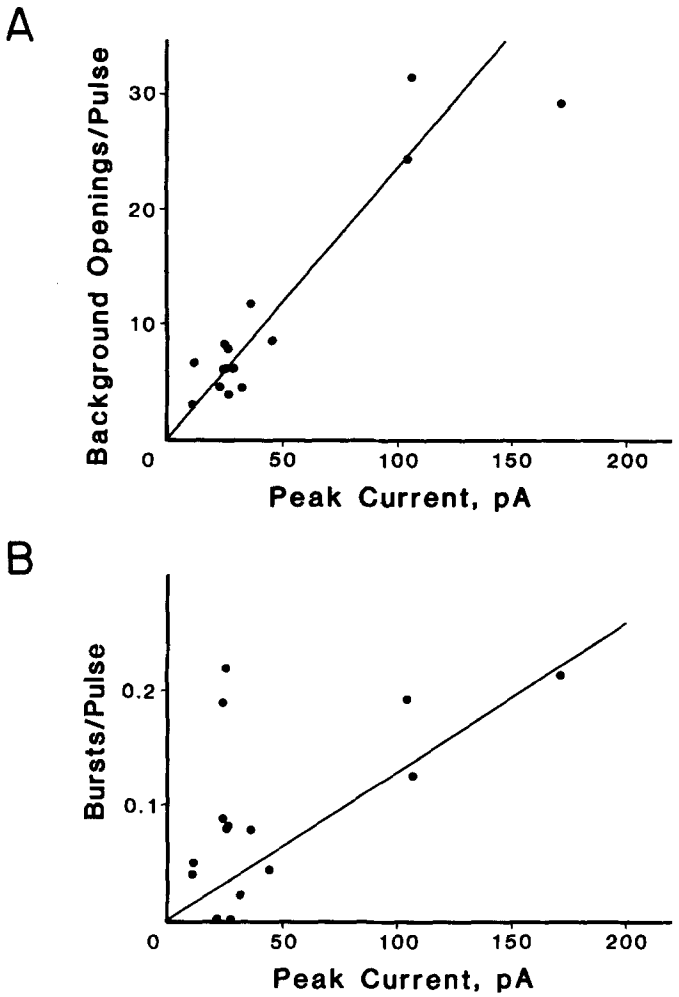

FIGURE 5. The frequency of occurrence of late currents and the early current amplitudes were correlated from patch to patch. (*A*) The average number of background openings during 400-ms pulses are plotted against the mean peak current at −20 mV for each of 15 patches that we studied. The data from pulses to −50 to −20 mV were included in the average frequencies because we saw no significant differences in the rates at each individual potential. (The average rate of appearance of background openings in five patches at the four potentials was as follows: −50, 0.25 ± 0.07; −40, 0.24 ± 0.05; −30, 0.25 ± 0.07; −20, 0.27 ± 0.08 openings per pulse per pA of peak early current.) The solid line is the linear regression that also passes through the origin. Its slope is 0.24 openings/pulse/pA early current. (*B*) The frequency of burst appearance during 400-ms pulses plotted against the mean peak current at −20 mV for the same 15 patches as in *A*. Data were lumped from all potentials. Bursts with durations <20 ms were neglected. Bursts that were interrupted by closed periods up to 50 ms were counted as a single burst, while those that appeared in sequential pulses were assumed to be different and were each counted. The solid line is a linear regression fit to the data, and has slope of 1.29×10^{-3} bursts/pulse/pA.

cant differences were seen in this frequency at the different pulse potentials (see figure legend), data from all pulses are lumped for each patch. The number of openings is plotted against the peak current during pulses to −20 mV from a holding potential of −120. The standard correlation coefficient, R (Bevington, 1969), for the two parameters had a value of 0.93, showing a significant correlation ($P \ll 0.001$) between the peak fast current and the appearance of background currents during each pulse.

The probability of observing a burst longer than 20 ms during each pulse was determined for each patch by counting the number of bursts and dividing by the number of pulses given. Since we saw no significant difference in this rate at the four potentials studied, our estimates lump observations from all potentials. This probability is plotted in Fig. 5*B* against the peak mean current at −20 mV for the same 15 patches as shown in Fig. 5*A*. Burst appearance is also correlated with the peak mean current. The correlation coefficient for burst probability vs. mean current was 0.56, which was also significant ($P < 0.05$).

The fast Na^+ currents in squid axon (Adleman and Palti, 1969; Rudy, 1978), skeletal muscle (Collins et al., 1982; Almers et al., 1983*b*), and other tissues undergo a slow inactivation process after prolonged depolarization. The onset and recovery of slow inactivation are on a time scale of seconds to minutes. In our preparation, a slow inactivation process appeared to affect both the background and the burst currents, as well as the fast Na^+ currents. When the membrane potential was held at −70 mV for several minutes, both the early and the background currents disappeared, and no bursts were observed. Furthermore, the frequency of both background and burst currents decreased during the 0.4-s test pulses. These findings are consistent with the hypothesis that a slow inactivation process affects all three types of current.

Our evidence shows that the early Na^+ currents and the late currents (background and burst) are all produced by channels with the same conductance and reversal potential. Furthermore, the magnitude of the late currents is proportional to that of the early currents, and both are affected by a slow inactivation process. We conclude that the two forms of late currents are produced by the same Na^+ channels that cause the early Na^+ currents.

Kinetic Properties of Background Currents

The individual channel openings that make up the background currents are very fast. Fig. 6, *A–D*, shows histograms compiled from all the nonbursting late events from one patch at the four pulse potentials. The distributions of channel open times were exponential in form, although in each case a small number of long openings could not be explained by the predominant component. Although we do not yet know the origin of these long openings, they might be the result of the limited resolution of our recordings for these very fast openings and closings. The time constants of the best-fitted single exponentials for these histograms are given in the figure. They all have similar magnitude, ranging from 0.27 ms at −50 mV to 0.23 ms at −20 mV. The time constant values for the background currents in other patches were similar. Although it is clear that the open time did not change strongly with membrane potential, our data are not sufficiently

precise to determine the exact potential dependence of the open times. The mean open times at all potentials were considerably faster than the rate of inactivation of the early mean currents, ~1.5–2 ms.

The distribution of closed times during pulses with only background current had two prominent exponential components, as shown in Fig. 7. If the background currents were caused by the activity of many independent channels, the slow component would represent the average interval between the openings of these different channels. This interpretation predicts that patches with large

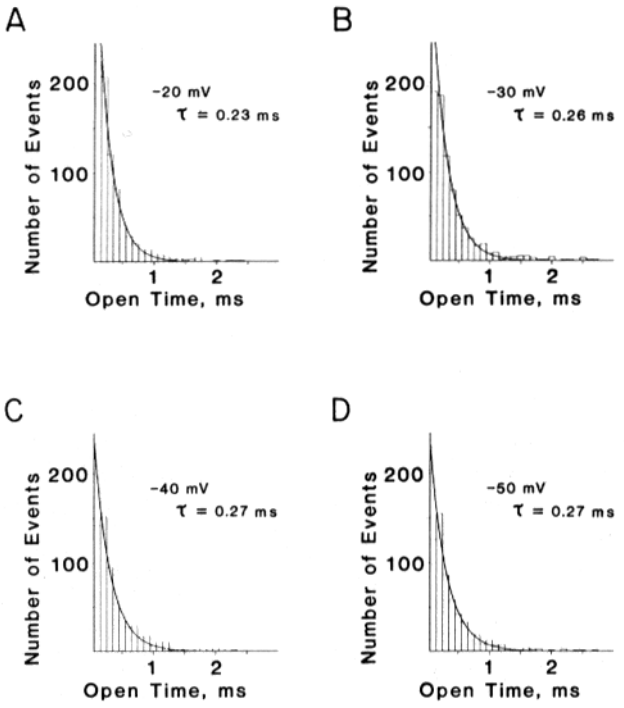

FIGURE 6. Open time distributions of background currents. (*A–D*) Open time histograms of the background currents recorded from one patch during 400-ms pulses to four different potentials (−20 to −50 mV) from a holding potential of −120 mV. The solid lines are the single exponentials best fitted to all bins but the first. The time constants of the exponentials ranged from 0.23 ms at −20 mV to 0.27 ms at −50 mV, as indicated in the figure.

peak early currents would have shorter intervals between openings. Our observations (see also Fig. 5*A*) support this interpretation.

The fast component of closed times had a time constant in the range of several hundred microseconds at all potentials studied. The simplest interpretation for the origin of this fast component is that each individual channel has the possibility of entering a closed but not inactivated state, and then quickly reopening, as has been shown for Na^+ channels during the early currents (Aldrich et al., 1983).

We have measured the tendency for channels to reopen during the background

activity as follows. We first made the assumption that the background current is due to channels that return occasionally from an inactivated state. When a channel opens after an extended quiescent period, it starts an "epoch" that ends when the channel re-enters the inactivated state. A channel that is open at the start of an epoch would then have two possible fates: it might close by inactivating again, in which case the epoch would include only one opening, or it might close

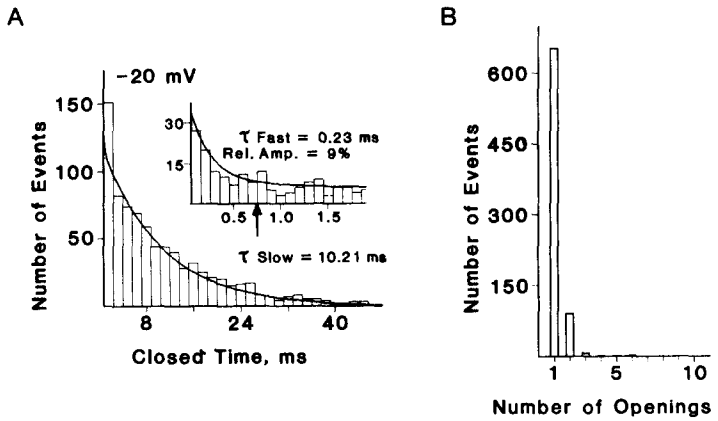

FIGURE 7. Closed time distributions and channel reopening during background currents. (*A*) Histogram of all closed times during 22 pulses to −20 mV in the same patch as used for Fig. 6. Two exponential components were present. The best-fitted sum of exponentials had a time constant of 10.2 ms for the slow component, probably corresponding to the average interval between the openings of independent channels (see text). The inset shows the fast component, which probably corresponds to the rapid reopening of individual channels, with higher temporal resolution. Its time constant was 0.23 ms; the relative area under the fast component was 9%. The arrow indicates the threshold interval used to count channel reopening. Sets of openings separated by intervals no longer than this interval were counted as reopenings of the same channel in *B*. The threshold duration was set so that the chance of missing an appropriate reopening was small and was equal to the chance of erroneously including the opening of a different channel in the set. (*B*) A histogram of the number of openings in each set or "epoch" delineated by the threshold interval shown in *A* (also see text). At −20 mV, 89% of all background epochs consisted of only one opening. The distributions at the three other potentials that we studied were similar: at −50, 86% had one, 12% had two, and 2% had three openings per epoch. At −40, 91% had one, 8% had two, and 1% had three openings per epoch. At −30, 93% had one, 7% had two, and 1% had three openings per epoch.

to some other state from which it could quickly reopen. In the latter case, the epoch would have two or more openings. Thus, the fast component of the closed time distribution measures the closings within epochs, whereas the slow time constant measures the intervals between epochs.

In practice, we defined an epoch as a set of openings that were separated from all other currents by intervals greater than a predetermined threshold, but which

included closings with a duration shorter than this threshold interval. We determined the magnitude of the threshold interval so that the probability of missing an opening that belonged in an epoch was small and equal to the probability of erroneously including openings from another channel in the epoch. For the data shown in Fig. 7, this threshold value was 0.7 ms, as indicated by the arrow in the inset of Fig. 7*A*. Fig. 7*B* shows a histogram of the number of openings in each epoch. 87% of all epochs had only one opening, 12% had two, 1% had three, etc. Thus, the average number of openings per epoch was ~1.2. Extending the threshold interval to 1.2 ms had little effect—84% of all epochs then had one opening. The number of openings per epoch also was not strongly affected by membrane potential (see the legend of Fig. 7).

Kinetics of Channel Openings During Bursts

The bursts of openings in the late currents consisted of tens to hundreds of openings, presumably from the same channel. The gating kinetics of an individual channel can thus be determined by measuring the open and closed time distributions during these bursts. Fig. 8, *A* and *B*, shows histograms of the observed open and closed time from one burst at −30 mV. Both are well fitted by single-exponential curves. The best-fitted time constant for the open time distribution was 0.84 ms, whereas that of the closed time distribution was 0.29 ms. We performed similar analyses for each individual burst that we observed. The resultant values for open and closed time constants are plotted as a function of membrane potential in Fig. 8*C*.

Fig. 8*C* shows that the best-fitted single exponential to either the open or closed times histograms varied considerably from burst to burst. This variation was not due to statistical uncertainties in the fitted parameters. The standard error for each of the parameters was, in general, <10% of its amplitude. The differences between the kinetics during individual bursts was considerably greater than 10%, which indicates that individual channels may be heterogeneous. (A more extensive statistical analysis of the open times during the bursts confirmed this heterogeneity between channels and showed that an individual channel may occasionally change its open time distribution during a single burst [Patlak et al., 1986]. These results indicate that the process that controls gating during bursts may also have modes. The reader is referred to the reference cited above for further information.)

At −40 mV, the open and closed times are about equal, with time constants in the range of 0.5 ms. Thus, the channel is open half the time when bursting at this potential. As the membrane is made more depolarized, the open times lengthen to 1–2 ms (at −20 mV), while the closed times shorten to <0.2 ms, giving bursts that are progressively more open than closed. However, openings and closings that were shorter than our maximum temporal resolution of 0.1 ms were not observed. The absence of these short events from our records leads to the biasing of the measured distributions toward longer times. Since both the mean open and closed times were close to the limit of resolution, this bias was significant and could not be corrected by standard algorithms (see Methods). Therefore, the time constant values shown in Fig. 8 must be interpreted as the

upper bounds for the actual time constants. For this reason, the extent of change in these time constants with membrane potential cannot yet be determined with precision.

In order to measure the voltage dependence of the channel's kinetics with much less bias, we measured the fraction of the total burst duration during which

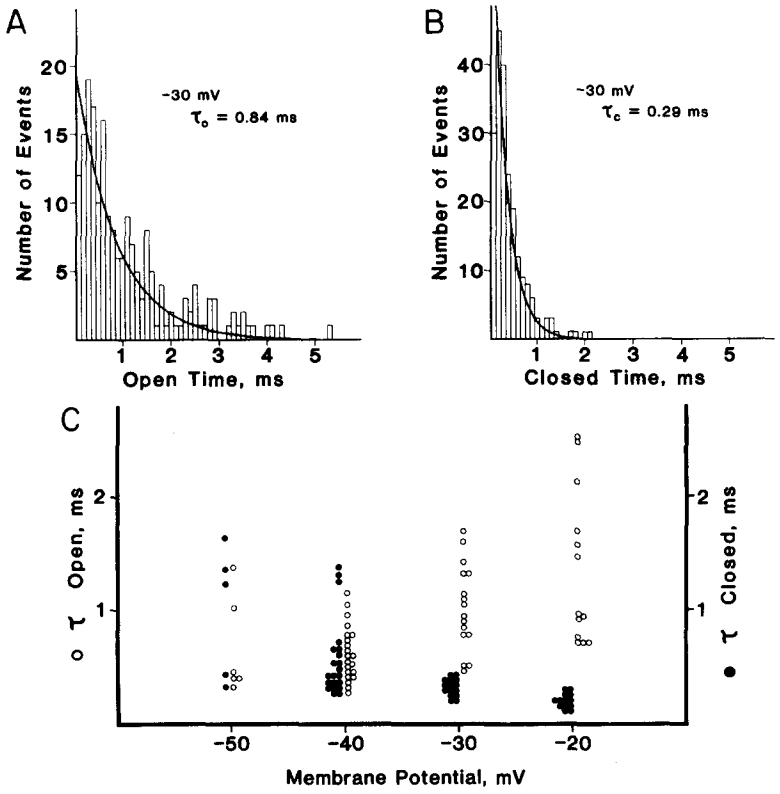

FIGURE 8. Open and closed time distributions of bursts. (*A*) Histogram of open times during one burst at −30 mV. The solid line is the best-fitted single exponential to these data. Its time constant was 0.84 ms. (*B*) Histogram of the closed times from the same burst as in *A*. The solid line is the best-fitted single exponential. Its time constant was 0.29 ms. (*C*) Voltage dependence of the best-fitted single-exponential time constants of the open and closed time distributions. Each open circle is the open time constant for one burst, and each solid circle is the closed time constant. The plotted values are not corrected for missed openings or closings (at our 0.1-ms resolution); they would be shifted to shorter times if such corrections were possible (see text).

the channel current was greater than half the current amplitude of the open channel. We determined this "fractional open time" for each individual burst. The points plotted in Fig. 9 are the mean and standard deviation of measurements from the bursts observed at four pulse potentials. The number of bursts at each point is given in parentheses in the figure. The data clearly show the

increasing tendency toward higher fractional open time with greater depolarization. At −50 mV, channels were 24% open during bursts, whereas at −20 mV, they were 86% open. Both the values of the measured open and closed time constants and the voltage dependence of the fractional open time during bursts are consistent with the hypothesis that bursts represent channels in which the normal inactivation fails to occur. This hypothesis will be considered further in the Discussion.

Exact measurement of the average burst length was not possible in our data because ~10–20% of all bursts lasted for the entire duration of the 0.4-s pulse. Furthermore, some bursts appeared to be interrupted by pauses of >20 ms, thus

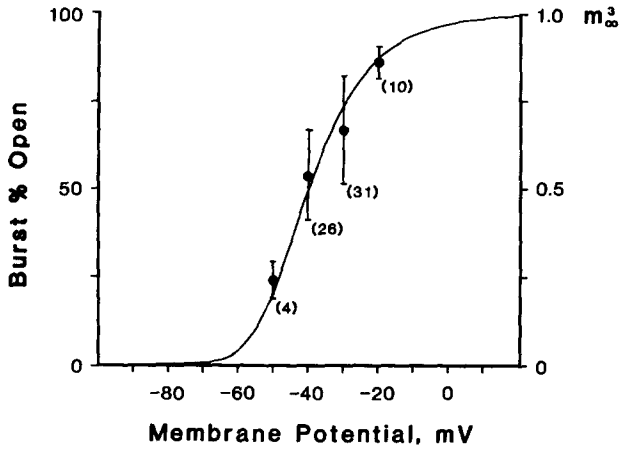

FIGURE 9. Voltage dependence of the fractional open time during bursts. The time spent above half of the unit amplitude was divided by the total duration for each individual burst. The mean ± standard deviation for all bursts measured at the four pulse potentials is plotted in the figure (the number of bursts at each potential is given in parentheses). At −50 mV, bursting channels were open 26% of the time; at −20 mV, they were open 86% of the time. The solid line in the figure is the value of m_∞^3 calculated using standard Hodgkin-Huxley (1952) kinetics. The voltage-dependent parameters for the fit were taken from the Campbell and Hille (1976) fits to the macroscopic Na^+ kinetics in frog muscle. The voltages from their fits have been shifted −13 mV in this plot because we worked at a lower Ca^{2+} concentration (see text).

complicating the definition of a burst. Nevertheless, our data permitted us to set a lower bound for the average length of bursts. The mean burst length was between 100 and 200 ms at the potentials that we studied. Since bursts appeared to be sensitive to the slow inactivation process of the Na^+ channel, the burst durations measured during 0.4-s test pulses may have been dominated by the rate of slow inactivation, not by the length of the burst mode itself. We have noticed a tendency for bursts to appear in sequential pulses, which implies that the bursting mode actually may have lasted for tens of seconds. Further measurements will be necessary to clarify this point.

DISCUSSION

This paper reports the first quantitative measurements of the single channel basis of the slowly inactivating and steady Na^+ current (referred to collectively as "late" currents). We saw two distinct categories of late Na^+ channel activity: the first was a background activity consisting of the isolated, very brief openings of many different channels, whereas the second consisted of prolonged bursts of openings from a single channel. Both types of activity provide valuable kinetic information about Na^+ channels.

There is little doubt that the late currents were due to activity of the same Na^+ channels that gave rise to the transient Na^+ currents at the start of the pulse. The unitary events had similar amplitude and reversal potential for the fast, the background, and the burst currents. The frequency of occurrence of the late events was correlated with the magnitude of the early currents. Finally, all three components disappear when the holding potential is sufficiently depolarized to cause slow inactivation of the channels. Although we have not demonstrated TTX sensitivity of the late currents (membrane patches in the outside-out configuration were not stable enough in this preparation), we feel that the evidence is sufficient to establish unequivocally the identity of the late current channel.

In order to emphasize the rarity of the late current events at the level of individual channels, we estimated the frequency with which any particular channel may have contributed to the background openings and the bursts (assuming that all channels are identical). We have fitted straight lines to the data in Fig. 5 to determine the rate of background openings per pulse, per picoampere of peak early current at −20 mV (Fig. 5*A*), and similarly for the rate of bursting (Fig. 5*B*). The abscissae of these graphs may be transformed from peak current to number of channels by estimating the number of channels necessary to give 1 pA of peak early current. From fluctuation analysis of 11 ensembles on eight patches, we estimated the single channel current to be 0.99 pA, and the peak probability of opening to be 0.40 (± 0.12). Thus, 1 pA peak current at −20 mV corresponded to 2.5 channels.

The slopes of the lines in Fig. 5, *A* and *B*, may therefore be transformed by dividing each by 2.5. This gives a frequency that a single channel will contribute a background opening during one pulse as 0.096 openings per pulse per channel. The frequency of bursting for a single channel during one pulse is 5.2×10^{-4} bursts per pulse per channel. In terms of observing events like those reported here, if one had an ideal patch containing one channel, a background event would be seen once during ~10 pulses (about once per 4 s of test pulse, ignoring slow inactivation). A burst would be seen approximately once every 2,000 pulses.

The fraction of the peak current that was carried by background openings can be calculated as follows: as determined above, at −20 mV, the peak probability of opening for a channel was ~0.4, and the single channel current was 0.99 pA. The peak current for one channel was thus 0.4 pA. One channel opened at late times every 4 s (neglecting slow inactivation), and remained open for 0.23 ms. The average number of openings was 1.2. The channel therefore was conducting for ~0.3 ms out of every 4 s. Its average background current was therefore 7.5×10^{-5} pA, or 0.02% of peak current.

The fraction of the peak current carried by bursts can be calculated in a similar manner: if the channel bursts once every 2,000 pulses, and it carries 0.99 pA 86% of the time during bursts at −20 mV, then the bursting current averages 4.2×10^{-4} pA, or 0.1% of peak current. Since the background currents at this potential were 0.75×10^{-4} pA, the bursts carry ~85% of late currents. This fraction decreased slightly at more hyperpolarized potentials because the fractional open time during bursts decreased.

The total late current is the sum of the background and burst contributions, or 0.12% of the peak current at −20 mV. Late currents of similar magnitude have been observed in squid giant axon under normal (Shoukimas and French, 1980) and perfused conditions (Chandler and Meves, 1970; Oxford and Yeh, 1985), in node of Ranvier (Dubois and Bergman, 1975), and in cardiac muscle (Gintant et al., 1984) in the range of potentials that we studied. The surprising aspect of our results is that most of the late current is carried by bursting channels. None of the hypotheses previously proposed to account for late currents predicted this type of activity.

The traditional explanation for late currents through Na^+ channels is that there is a range of potentials over which neither the steady state activation nor inactivation parameters, m_∞ and h_∞, is zero (Hodgkin and Huxley, 1952; McAllister et al., 1975; Attwell et al., 1979). Although this hypothesis can explain steady currents over a narrow range near the threshold potential, it is not adequate to explain the relatively large steady currents seen after strong depolarization (Shoukimas and French, 1980), and in altered intracellular ionic environments (Chandler and Meves, 1970; Bezanilla and Armstrong, 1977; Oxford and Yeh, 1985). An alternative hypothesis uses a second open state, connected directly to the inactivated state, to explain late currents (Chandler and Meves, 1970; Bezanilla and Armstrong, 1977; Sigworth, 1981). Our data provide a means of testing these hypotheses, since each leads to specific predictions of the underlying single channel activity.

For example, if channels operate by switching reversibly between different states (i.e., the standard Markov chain assumptions; see French and Horn, 1983), then a channel that returns from inactivation to the normal open state would have kinetics similar to those during the early currents. Aldrich et al. (1983) demonstrated that the early Na^+ channel currents in tissue-cultured neuroblastoma cells consisted of openings that were much shorter than the rate of inactivation of the mean currents. The mean open times were shown to be insensitive to membrane potential, and each channel usually opened only once. Therefore, the late openings of such channels would consist of isolated short openings whose mean lifetime was insensitive to membrane potential.

The bursts of Na^+ currents clearly do not fit this prediction. On the other hand, the background currents have many properties in common with the predictions of the Aldrich et al. model. They occur as isolated open events with but a slight tendency to reopen, and their mean open time is short and insensitive to membrane potential. While our observations lend support to both the Aldrich et al. model and the hypothesis that the background currents are due to the activity of normal Na^+ channels, we cannot support them unequivocally: our observation that there is little voltage dependence in the frequency of back-

ground openings is contrary to the predictions of most Na^+ channel models, which show an increasing rate of return from inactivation as the membrane potential becomes more hyperpolarized. Further experiments will be necessary to prove or disprove the hypothesis that the background currents are due to normal Na^+ channels that return from inactivation.

Hypotheses that use a second open state of the Na^+ channel to explain the late current predict that the late single channel currents would be isolated openings, presumably with a longer mean open time. These predictions do not fit our observation of bursting currents. In order to explain the repeated reopening of the channel during a burst, additional closed states must be incorporated into such models. Although such additions would improve these second-open-state models, we believe that they add unnecessary complexity. We hypothesize instead that bursts are due to the entry of the channel into a kinetic "mode" that is characterized by the reversible failure of the channel's inactivation gate for prolonged periods.

Since the observations of bursting activity of the Na^+ channel are new, it is first important to examine whether bursting is a normal, ubiquitous property of Na^+ channels, or whether it was produced as an artifact of our recordings. Since our recordings were from cells that had undergone enzyme treatment, the bursts might have been due to degradation of the channel. However, we have also seen bursts in tissue-cultured rat skeletal muscle that have not undergone enzyme treatment (Patlak and Ortiz, 1985*a*), and they have been seen as well in cultured pituitary cells of the GH3 line (Horn, R., and C. Vandenberg, personal communication). These observations indicate that the appearance of bursts is independent of enzyme treatment. Our recordings were also made on cells that were internally dialyzed. This cannot have caused the bursting activity since we have also seen bursts using cell-attached recordings in cardiac (Patlak and Ortiz, 1985*b*) and skeletal muscle cells (unpublished observations) that were intact.

Bursts might be the result of interaction between Na^+ channels and the glass of the patch electrode, which is in close contact with the membrane at the edge of the patch. Although we have no other direct method of observing bursts, their presence may be detectable in standard voltage-clamp recordings of late Na^+ currents. Fluctuation analysis by Sigworth (1981) and by Conti et al. (1980) in node of Ranvier show slow kinetic components in the late Na^+ currents that are not explained by standard models of the channel's kinetics. This slow activity could have been caused by burst-like kinetics, which indicates that Na^+ channel bursting may also occur under standard voltage-clamp conditions.

If bursts are not caused by our experimental procedures, then they are probably due to spontaneous, reversible changes in the function of the channel. Several other types of channel have been shown to reversibly change their kinetic activity. Glutamate-activated channels spontaneously changed both their opening and closing kinetics after treatment with concanavalin A (Patlak et al., 1979). Acetylcholine channels also appear to undergo shifts in their kinetics (Auerbach and Lingle, 1985), and Hess et al. (1984) have shown that Ca channels have several kinetic modes of activity. Furthermore, Na^+ channels have been shown to hibernate (Horn et al., 1984) and to undergo sudden alterations in the kinetics

of their activation gates after treatment with batrachotoxin (Moczydlowski et al., 1984; Weiss et al., 1984).

The inactivation gate of the Na^+ channel is relatively labile. Inactivation is quickly removed by proteolytic treatment of the membrane's cytoplasmic face (Armstrong et al., 1973). Furthermore, the magnitudes of the late currents are dramatically modified by the internal ionic environment of the membrane (Oxford and Yeh, 1985). Such observations, as well as our own, might be explained as follows. The inactivation gate may occasionally switch between functional and nonfunctional modes. The rate constants of this switching reaction normally would favor the functional mode, but might be influenced by ionic environment, membrane potential, and proteolytic enzymes.

The kinetics of the Na^+ activation gating (i.e., current onset) are not strongly affected by removal of inactivation (Oxford, 1981; Patlak and Horn, 1982). This observation is consistent with the hypothesis that the activation gating of the channel controls the latency to first event, whereas the inactivation process is the primary determinant of channel lifetime (Aldrich et al., 1983). Therefore, if bursting behavior were due to a spontaneous loss of function of the inactivation gate, then the kinetics of the openings and closings within a burst would represent the activation gating of the channel. A comparison of the channel kinetics during bursts with that expected for normal Na^+ channels with inactivation removed would provide an important test of this hypothesis.

As shown in Fig. 9, the fractional open time of the channel during bursts increased with depolarization, as expected for Na^+ channels without inactivation. In order to further explore this similarity, we have calculated the fractional open time of the activation gates that would be predicted by a Hodgkin-Huxley model of Na^+ channel kinetics. If inactivation were removed (by pronase or *N*-bromoacetamide, for example), this parameter would represent the fractional open time of the channel, and could be compared directly with our data. Campbell and Hille (1976) fitted the macroscopic Na^+ currents from skeletal muscle of the same frog species as we used in our studies. Using the Hodgkin-Huxley (1952) model, they determined the constants necessary to calculate α_m and β_m as a function of membrane potential. The activation parameter, m_∞, can be calculated as:

$$m_\infty = \alpha_m/(\alpha_m + \beta_m).$$

m_∞^3 is then a measure of the fractional open time of a noninactivating Na^+ channel.

Our recordings were made at an extracellular calcium concentration lower than that used by Campbell and Hille when they determined their model parameters. However, they also showed that reduction of the Ca causes an increase in the surface potential on one side of the membrane, and thus a hyperpolarizing shift in the transmembrane potential. They showed (Fig. 5 of Campbell and Hille, 1976) that at 0.2 mM Ca, the concentration that we used for our study, the currents could be fitted by shifting the membrane potential by −13 mV. We have therefore shifted the membrane potentials used to determine α_m and β_m by 13 mV in order to compare their fits to our data. The solid

curve in Fig. 9 is the result of this calculation. Our data are very well fitted by the curve derived from the Campbell-Hille measurements assuming a simple loss of inactivation.

Further support for the hypothesis that bursting represents a loss of inactivation comes from the observation that the mean open time of the bursting channel is longer than during the background current, and is voltage dependent. The mean open time of Na^+ currents is prolonged after enzymatic removal of inactivation, and it is voltage dependent (Patlak and Horn, 1982; Vandenberg and Horn, 1984). Higher-resolution recordings of Na^+ channel bursts and a demonstration that the process is reversible for an individual channel will further strengthen this interpretation.

The use of proteolytic enzymes to remove inactivation has become a well-established technique for the study of Na^+ channel kinetics. One problem with such experiments is the potential for nonspecific effects of the enzymes on the channel and the membrane. If the bursts that we observed do represent a spontaneous loss of inactivation, then the kinetics of the channel during a burst provide an independent measurement of the rates of transition between the resting and the open state, without the possibility that enzymes have caused extraneous channel damage.

When such measurements of gating kinetics during bursts are combined with the measurement of background current kinetics, most of the rate constants necessary to predict the form and magnitude of the early currents can be obtained. A comparison of the predicted and the actual currents will provide an additional test of our hypotheses for background and burst kinetics. Although such an analysis is beyond the scope of the presented paper, its possibility demonstrates the power of recording from patches with large numbers of channels.

The authors wish to thank Ms. Margaret Bolton for expert technical assistance, and Drs. R. Horn, D. Warshaw, and W. Gibbons for comments on the manuscript.

This work was supported in part by a Grant-in-Aid from the American Heart Association (AHA) with funds contributed in part by its Vermont Affiliate. Dr. Patlak is an Established Investigator of the AHA. Dr. Ortiz is an Agan fellow of the AHA Vermont Affiliate.

Original version received 29 July 1985 and accepted version received 4 November 1985.

REFERENCES

Adelman, W. J., and Y. Palti. 1969. The effects of external potassium and long duration voltage conditioning on the amplitude of sodium currents in the giant axon of the squid, *Loligo pealei*. *Journal of General Physiology*. 54:589–606.

Aldrich, R. W., D. P. Corey, and C. F. Stevens. 1983. A reinterpretation of mammalian sodium channel gating based on single channel recording. *Nature*. 306:463–440.

Almers, W., P. R. Stanfield, and W. Stuhmer. 1983*a*. Lateral distribution of sodium and potassium channels in frog skeletal muscle: measurements with a patch clamp technique. *Journal of Physiology*. 336:261–284.

Almers, W., P. R. Stanfield, and W. Stuhmer. 1983*b*. Slow changes in currents through sodium channels in frog sarcolemma. *Journal of Physiology*. 339:253–271.

Armstrong, C. M., F. Bezanilla, and E. Rojas. 1973. Destruction of sodium conductance inactivation in squid axons perfused with pronase. *Journal of General Physiology.* 62:375–391.

Attwell, D., I. Cohen, D. Eisner, M. Ohba, and C. Ojeda. 1979. The steady state TTX-sensitive ("window") sodium current in cardiac Purkinje fibres. *Pflügers Archiv European Journal of Physiology.* 379:137–142.

Auerbach, A., and C. Lingle. 1985. Heterogeneous burst kinetics of *Xenopus* acetylcholine receptor channels at high agonist concentrations. *Biophysical Journal.* 47:41*a*. (Abstr.)

Bevington, P. R. 1969. Data Reduction and Error Analysis for the Physical Sciences. McGraw-Hill, New York. 119–133.

Bezanilla, F., and C. M. Armstrong. 1977. Inactivation of the sodium channel. I. Sodium current experiments. *Journal of General Physiology.* 70:549–566.

Campbell, D. T., and B. Hille. 1976. Kinetic and pharmacological properties of the sodium channel of frog skeletal muscle. *Journal of General Physiology.* 67:309–323.

Carmeliet, E. 1984. Slow inactivation of the sodium current in rabbit cardiac Purkinje fibres. *Journal of Physiology.* 353:125p. (Abstr.)

Chandler, W. K., and H. Meves. 1970. Evidence for two types of sodium conductance in axons perfused with sodium fluoride solution. *Journal of Physiology.* 211:653–678.

Collins, C. A., E. Rojas, and B. A. Suarez-Isla. 1982. Activation and inactivation characteristics of the sodium permeability in muscle fibres from *Rana temporaria*. *Journal of Physiology.* 324:297–318.

Colquhoun, D., and F. J. Sigworth. 1983. Fitting and statistical analysis of single channel records. *In* Single Channel Recording. B. Sakmann and E. Neher, editors. Plenum Publishing Co., New York and London. 191–263.

Conti, F., B. Neumcke, W. Nonner, and R. Stampfli. 1980. Conductance fluctuations from the inactivation process of sodium channels in myelinated nerve fibres. *Journal of Physiology.* 308:217–239.

Dubois, J. M., and C. Bergman. 1975. Late sodium current in the node of Ranvier. *Pflügers Archiv European Journal of Physiology.* 357:145–148.

French, R. J., and R. Horn. 1983. Sodium channel gating: models, mimics, and modifiers. *Annual Review of Biophysics and Bioengineering.* 12:319–356.

Gintant, G. A., N. B. Datyner, and I. S. Cohen. 1984. Slow inactivation of a tetrodotoxin-sensitive current in canine cardiac Purkinje fibers. *Biophysical Journal.* 45:509–512.

Hamill, O. P., A. Marty, E. Neher, B. Sakmann, and F. J. Sigworth. 1981. Improved patch clamp techniques for high-resolution current recording from cells and cell-free membrane patches. *Pflügers Archiv European Journal of Physiology.* 391:85–100.

Hess, P., J. B. Lansman, and R. W. Tsien. 1984. Different modes of Ca channel gating behaviour favoured by dihydropiridine Ca agonists and antagonists. *Nature.* 311:538–544.

Hille, B., and D. T. Campbell. 1976. An improved vaseline gap voltage clamp for skeletal muscle fibers. *Journal of General Physiology.* 67:265–293.

Hodgkin, A. L., and A. F. Huxley. 1952. A quantitative description of membrane current and its application to conduction and excitation in nerve. *Journal of Physiology.* 117:500–544.

Horn, R., C. A. Vandenberg, and K. Lange. 1984. Statistical analysis of single sodium channels: effects of *N*-bromoacetamide. *Biophysical Journal.* 45:323–335.

McAllister, R. E., D. Noble, and R. W. Tsien. 1975. Reconstruction of the electrical activity of cardiac Purkinje fibres. *Journal of Physiology.* 251:1–59.

Moczydlowski, E., S. S. Garber, and C. Miller. 1984. Batrachotoxin-activated Na channels in planar lipid bilayers. Competition of tetrodotoxin block by Na. *Journal of General Physiology.* 84:665–686.

Neher, E. 1983. The charge carried by single-channel currents of rat cultured muscle cells in the presence of local anaesthetics. *Journal of Physiology.* 339:663–678.

Oxford, G. S. 1981. Some kinetic and steady-state properties of sodium channels after removal of inactivation. *Journal of General Physiology.* 77:1–22.

Oxford, G. S., and J. Z. Yeh. 1985. Interactions of monovalent cations with sodium channels in squid axon. I. Modification of physiological inactivation gating. *Journal of General Physiology.* 85:583–602.

Patlak, J. B., K. A. F. Gration, and P.N. R. Usherwood. 1979. Glutamate-activated channels in locust muscle. *Nature.* 287:643–646.

Patlak, J., and R. Horn. 1982. The effect of *N*-bromoacetamide on single sodium channel currents in excised membrane patches. *Journal of General Physiology.* 79:333–351.

Patlak, J., and M. Ortiz. 1985*a*. Slow currents through skeletal muscle Na channels are not "window currents." *Biophysical Journal.* 47:190*a*. (Abstr.)

Patlak, J., and M. Ortiz. 1985*b*. Slow currents through single sodium channels of the adult rat heart. *Journal of General Physiology.* 86:89–104.

Patlak, J., M. Ortiz, and R. Horn. 1986. Open time heterogeneity during bursting of sodium channels in frog skeletal muscle. *Biophysical Journal.* In press.

Rakowski, R. F., P. De Weer, and D. C. Gadsby. 1985. Threshold channel can account for steady-state TTX-sensitive sodium current of squid axon. *Biophysical Journal.* 47:31*a*. (Abstr.)

Reuter, H. 1968. Slow inactivation of currents in cardiac Purkinje fibres. *Journal of Physiology.* 197:233–253.

Roberts, W. M., and W. Almers. 1985. Increased Na current density near endplates in snake skeletal muscle. *Biophysical Journal.* 47:189*a*. (Abstr.)

Rudy, B. 1978. Slow inactivation of the sodium conductance in squid giant axons. Pronase resistance. *Journal of Physiology.* 283:1–21.

Shoukimas, J. J., and R. J. French. 1980. Incomplete inactivation of sodium currents in nonperfused squid axon. *Biophysical Journal.* 32:857–862.

Sigworth, F. J. 1980. The variance of sodium current fluctuations at the node of Ranvier. *Journal of Physiology.* 307:97–129.

Sigworth, F. 1981. Covariance of nonstationary sodium current fluctuations at the node of Ranvier. *Biophysical Journal.* 34:111–133.

Sigworth, F. J., and E. Neher. 1980. Single Na channel currents observed in rat muscle cells. *Nature.* 287:447–449.

Stuhmer, W., W. M. Roberts, and W. Almers. 1983. The loose patch clamp. *In* Single Channel Recording. B. Sakmann and E. Neher, editors. Plenum Publishing Co., New York and London. 123–132.

Vandenberg, C. A., and R. Horn. 1984. Inactivation viewed through single sodium channels. *Journal of General Physiology.* 84:535–564.

Weiss, L. B., W. N. Green, and O. S. Andersen. 1984. Single-channel studies on the gating of batrachotoxin (BTX)-modified sodium channels in lipid bilayers. *Biophysical Journal.* 45:67*a*. (Abstr.)